Critical behavior of the random-bond Ashkin-Teller model: A Monte Carlo study

Shai Wiseman* and Eytan Domany†

Department of Physics of Complex Systems, Weizmann Institute of Science, Rehovot 76100 Israel

(Received 19 October 1994)

The critical behavior of a bond-disordered Ashkin-Teller model on a square lattice is investigated by intensive Monte Carlo simulations. A duality transformation is used to locate a critical plane of the disordered model. This critical plane corresponds to the line of critical points of the pure model, along which critical exponents vary continuously. Along this line the scaling exponent corresponding to randomness $\phi = (\alpha/\nu)$ varies continuously and is positive so that randomness is relevant, and different critical behavior is expected for the disordered model. We use a cluster algorithm for the Monte Carlo simulations based on the Wolff embedding idea, and perform a finite size scaling study of several critical models, extrapolating between the critical bond-disordered Ising and bond-disordered four-state Potts models. The critical behavior of the disordered model is compared with the critical behavior of an anisotropic Ashkin-Teller model, which is used as a reference pure model. We find no essential change in the order parameters' critical exponents with respect to those of the pure model. The divergence of the specific heat C is changed dramatically. Our results favor a logarithmic type divergence at T_c, $C \sim \log L$ for the random-bond Ashkin-Teller and four-state Potts models and $C \sim \log \log L$ for the random-bond Ising model.

PACS number(s): 05.50.+q, 75.50.Lk, 75.40.Mg, 75.10.Nr

I. INTRODUCTION

How is critical behavior affected by the introduction of disorder (usually dilution or bond randomness) into a model? The Harris criterion [1–3] states that ϕ, the scaling index of the operator corresponding to randomness at the pure system fixed point (also called the crossover exponent) is equal to $\frac{\alpha}{\nu}$ (α and ν are the specific-heat and correlation length exponents of the pure model). Thus the critical behavior of the pure system is unaltered by disorder if $\alpha < 0$, and altered when $\alpha > 0$. If $\alpha = 0$ the situation is marginal.

Renormalization-group methods (namely expansion in the parameter $\epsilon = 4 - d$, where d is the dimensionality), applied to n-component continuous spin models with weak quenched bond disorder [4], confirmed the Harris criterion $\phi = \frac{\alpha}{\nu}$. Moreover, it was found that for $n < n_c = 4 - 4\epsilon + O(\epsilon^2)$ a new stable random fixed point with new exponents appears. For the case $n = 1$ (Ising model) the stability of an $O(\epsilon^{1/2})$ random fixed point was shown by Jayaprakash and Katz [5]. For the $d = 2$ Ising model, $\alpha = 0$, and the operator corresponding to randomness is expected to be marginally relevant.

Two partially conflicting theories by Dotsenko and Dotsenko [6] (DD) and by Shalaev [7], Shankar [8], and Ludwig [9] (SSL) were suggested for the $d = 2$ Ising model with small randomness. While both theories agreed on the divergence of the specific heat, e.g.,

$$C_{\text{imp}}(t) \sim \ln \ln 1/|t|, \tag{1}$$

conflicting predictions were made for other quantities like the magnetization M and susceptibility χ. Extensive Monte Carlo (MC) simulations of dilute and random-bond Ising models (see a review in Ref. [10] and references therein) helped to confirm the prediction on the specific heat. The other quantities were seen to behave (as predicted by SSL), in essence, as in the pure model. The disordered $d = 3$ Ising model has been studied by means of MC simulations as well [10].

Less attention has been paid in recent times to other disordered systems such as random q-state Potts models. Kinzel and Domany [3] used a real-space Migdal-Kadanoff renormalization transformation for the random-bond Potts model on the square lattice in two dimensions and found (when $\alpha_{pure} > 0$) a stable random fixed point with a reduced (with respect to the pure model) but positive α_{random}. Using methods of the same spirit, Andelman and Berker [11] also found a random fixed point. For $q = 4$ their calculation suggests $\alpha = -0.37$ and $\nu = 1.19$. Other workers [12,13] too have suggested a negative α for $q > 2$ Potts models in two dimensions. MC work on random q-state Potts models has not been carried out, except for recent work on the bond-random two dimensional eight-state Potts model [14], where randomness was shown to change the first order phase transition of the pure model into a second order one [15]. Novotny and Landau (NL) [16] used MC simulations to study the two dimensional site-dilute Baxter-Wu [17] model which is of the same universality class as the four-state Potts model. NL measured the exponents $\alpha = 0.0(2)$, $\nu = 1.00(7)$, and $\gamma = 1.95(8)$ which did not seem to depend on the amount of dilution. They could not determine whether the new stable fixed point

---

*Electronic address: shai@elect1.weizmann.ac.il
†Electronic address: fedomany@WEIZMANN.
weizmann.ac.il

is a $d = 2$ random Ising fixed point (which is very similar to the pure Ising fixed point) or a new impure Baxter-Wu fixed point.

In this paper we address the effect of randomness on a critical line which connects the critical points of the d =two Ising and four-state Potts models. Such is the critical line of the two dimensional Ashkin-Teller model [18] on a square lattice.

A convenient representation of the pure Ashkin-Teller (AT) model is in terms of two Ising spin variables, σ_i and τ_i, placed on every site of a lattice. Denoting by $\langle i, j \rangle$ a pair of nearest neighbor sites, the Hamiltonian is given by

$$\mathcal{H} = - \sum_{\langle i,j \rangle} [K\sigma_i\sigma_j + K\tau_i\tau_j + \Lambda\sigma_i\sigma_j\tau_i\tau_j] \qquad (2)$$

Here K is the strength of the interactions between neighboring σ and τ spins, and Λ is a four-spin coupling (throughout this paper we absorb a factor of $1/k_BT$ into the coupling constants). The phase diagram of the ferromagnetic AT model is known in two dimensions from duality transformations and renormalization group studies [19,20]. The three dimensional model has been studied as well [21]. The phase diagram which we reviewed previously [22] includes a line of critical points which connects the Ising critical point at one end to the four-state Potts critical point at the other end. Along this line the exponents vary continuously, and have been determined analytically [23,24], interpolating between their Ising and four-state Potts values. For instance, the crossover exponent connected with randomness $\phi = \frac{\alpha}{\nu}$ changes smoothly from 0 at the decoupled Ising point, to 1 at the four-state Potts point. Therefore, according to the Harris criterion, we expect randomness to be a relevant operator of varying strength in this regime of the AT model, and expect the critical behavior of the disordered model to differ from that of the pure model.

The critical behavior of the disordered AT model has not been studied before, to our knowledge, apart from a conjecture by Alcaraz and Tsallis [25] as to the location of the critical manifold of the bond dilute AT model. Nonetheless the effect of disorder on the critical line of the Baxter (or symmetric eight-vertex) model [26], which is isomorphic to the critical line of the AT model [23,24], was considered. DD [27] extended their study of the disordered Ising model to the Baxter model, and found, for small disorder, the specific-heat divergence to change from its pure form to the form of Eq. (1). Matthews-Morgan, Landau, and Swendsen (MLS) [28] studied the site-dilute Baxter model by means of a MCRG (MC renormalization-group) method. MLS found $\frac{1}{\nu} = y_T = 0.98(7)$ and $\frac{\gamma}{\nu}$ slightly below the Ising value. Both studies indicate that continuous variation of critical exponents of the pure model is substituted by flow to a random Ising fixed point.

In a previous paper [22] we described an efficient MC cluster algorithm [29] for the AT model. In this work we have used this algorithm to perform extensive MC simulations [30] of the random-bond AT model. The importance of using a cluster algorithm for the acquirement

of reasonably accurate data cannot be overlooked. This is especially true in the highly random regime where local algorithms are extremely slow [31] while cluster algorithms are most efficient [32,33]. The partial elimination of critical slowing down allows us to go to large lattice sizes (up to L=256) and obtain accurate results on the finite size scaling of the thermodynamic quantities at criticality. Our results seem to favor an Ising-like critical behavior.

This work is organized as follows. In Sec. II we define the random-bond AT model and a related anisotropic AT model. As will be explained, the anisotropic AT model is used as a nondisordered reference model for the random-bond model. We use the duality transformation of the AT model to locate exactly critical surfaces of the two models, which are related to the line of critical points of the pure model. In Sec. III we describe the MC cluster algorithm, give definitions of the measured quantities and describe our choice of simulation points. We have performed simulations of the anisotropic and random-bond AT models at several points on their critical surface. In Sec. IV we give our results, which consist of the finite size dependence of thermodynamic quantities of the two models at criticality. Analysis of our results shows that the anisotropic model exhibits varying critical exponents, i.e., the specific heat diverges as

$$C(t) \sim |t|^{-\alpha}, \qquad (3)$$

where at different points of the critical surface of the anisotropic AT model we measured different values of α. On the other hand, the random-bond model seems to exhibit a single type of behavior, i.e., the specific heat diverges as

$$C_{\text{imp}}(t) \sim -\ln|t|. \qquad (4)$$

This is identical to a pure Ising behavior and not to a random Ising one. In Sec. V we summarize our results.

II. DEFINITION OF MODELS AND LOCATION OF CRITICAL PLANES

The model we wish to study is the random-bond AT model (RBAT) on a square lattice, which is defined by the Hamiltonian

$$\mathcal{H} = - \sum_{\langle i,j \rangle} [K_{i,j}\sigma_i\sigma_j + K_{i,j}\tau_i\tau_j + \Lambda_{i,j}\sigma_i\tau_i\sigma_j\tau_j] . \qquad (5)$$

The coupling constants $K_{i,j}$ and $\Lambda_{i,j}$ are chosen according to

$$(K_{i,j}, \Lambda_{i,j}) = \begin{cases} (K^1, \Lambda^1) & \text{with probability } p \\ (K^2, \Lambda^2) & \text{with probability } 1 - p. \end{cases} \qquad (6)$$

It seems quite natural (the need for this comparison will be made clear at the end of this section) to compare the RBAT with the anisotropic AT model (AAT) with the same Hamiltonian (5) but with the couplings distributed as follows:

$$(K_{i,j}, \Lambda_{i,j}) = \begin{cases} (K^1, \Lambda^1) & \text{for bonds } (i,j) \text{ in the horizontal direction} \\ (K^2, \Lambda^2) & \text{for bonds } (i,j) \text{ in the vertical direction .} \end{cases} \tag{7}$$

Spatial anisotropy is usually known to be an irrelevant operator, that is, the critical behavior of a model is unaltered by the introduction of anisotropy. Thus one expects that continuous variation of critical exponents will continue to exist on some critical manifold of the AAT, as is the case for the isotropic (or pure) model.

A duality transformation can be used to locate critical manifolds of the AAT and RBAT in a way we now present.

A. Duality and location of a phase transition

Consider an AT system on a square lattice with spatially varying coupling constants (the spatial variation can be due to anisotropy, or it can be due to randomness as we consider below). The dual lattice D of the original square lattice G is the square lattice whose sites are at the centers of the plaquettes of the original lattice. In Fig. 1, sites of G are denoted by dots, while sites of D are denoted by crosses. Consider a bond of strength (K, Λ) between two sites in G. Under duality it is mapped onto a bond of strength $(\widetilde{K}, \widetilde{\Lambda}) = \vec{D}[(K, \Lambda)]$, where $\vec{D}$ is the duality transformation of the AT model [34,20] which we list in the Appendix. The dual bond lies in the dual lattice D, intersecting the original bond. This situation is depicted in Fig. 1. The original bond of strength (K, Λ) is depicted by the solid line while its dual is depicted by the dashed line.

Suppose the only spatial variation of the couplings is one of anisotropy. Then an AT system with couplings of strength (K^1, Λ^1) in the horizontal direction and strength (K^2, Λ^2) in the vertical direction, transforms under duality into an AT system on the dual lattice D with couplings of strength $(\widetilde{K^1}, \widetilde{\Lambda^1})$ in the vertical direction and strength $(\widetilde{K^2}, \widetilde{\Lambda^2})$ in the horizontal direction. The free energies of the original system and its dual have the same singular part, and therefore we can write

$$f_s[(K^1, \Lambda^1), (K^2, \Lambda^2)] = f_s[(\widetilde{K^2}, \widetilde{\Lambda^2}), (\widetilde{K^1}, \widetilde{\Lambda^1})] , \tag{8}$$

where the first pair of couplings corresponds to the horizontal bonds, and the second pair to the vertical ones. The duality transformation $\vec{D}$ is self-inverse. Thus an anisotropic AT system with couplings $[(K^1, \Lambda^1), (K^2, \Lambda^2)]$ such that $(K^2, \Lambda^2) = (\widetilde{K^1}, \widetilde{\Lambda^1})$, transforms under duality onto itself. So there exists a two dimensional self-dual manifold (it would help the reader to view the duality transformation as a mathematical mapping in the four dimensional space of couplings $[(K^1, \Lambda^1), (K^2, \Lambda^2)]$).

The line of critical points of the isotropic AT model lies within the subspace Σ, defined by $0 \leq \Lambda \leq K$. Σ is located between a decoupled Ising model where $\Lambda = 0$ and a four-state Potts model with $\Lambda = K$. Two subareas of Σ which map onto each other under duality are separated by a self-dual line [fulfilling $(K, \Lambda) = (\widetilde{K}, \widetilde{\Lambda})$]. The assumption that Σ contains only two phases, with a single phase transition between them (where f_s is nonanalytic) leads to the conclusion that this phase transition must occur on the self-dual line. In this way the line of critical points of the isotropic AT was located exactly [19].

Let us now consider the corresponding subspace Σ_A of the AAT, for which $0 \leq \Lambda^1 \leq K^1$ and $0 \leq \Lambda^2 \leq K^2$. Σ_A lies between an anisotropic decoupled Ising subspace where $\Lambda^1 = \Lambda^2 = 0$ and an anisotropic four-state Potts subspace with $\Lambda^1 = K^1$, $\Lambda^2 = K^2$. Σ_A is invariant under duality since for $0 \leq \Lambda \leq K$ we obtain (see the Appendix) $0 \leq \widetilde{\Lambda} \leq \widetilde{K}$. It follows also that the self-dual plane $0 \leq \Lambda^1 \leq K^1$, $(K^2, \Lambda^2) = (\widetilde{K^1}, \widetilde{\Lambda^1})$ is included in the subspace we are considering. Thus, again assuming that Σ_A contains only two phases, with a single phase transition between them, we conjecture that the self-dual plane is a plane of phase transitions (this kind of argument was first used by Fisch [35] for the random-bond Ising model, and later for Potts models by Kinzel and Domany [3]). Since the space of couplings is four dimensional, while the self-dual plane is only two dimensional, the self-dual plane is only part of the three dimensional critical manifold in Σ_A. Notice that this is unlike the case of the Potts model or any model with a single coupling constant, where the self-dual line is identical to the critical line.

B. A critical plane of the RBAT

The argument that leads to locating the corresponding critical plane of the RBAT is very similar to the one presented above, up to a subtle difference. Consider a
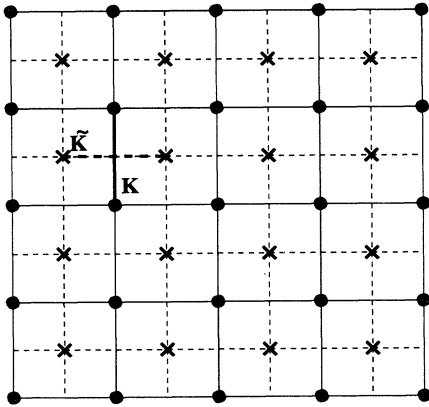

FIG. 1. The original lattice G is denoted by solid lines, while its sites are denoted by dots. The dual lattice D is denoted by dashed lines, while its sites are denoted by crosses. A bond of strength K is denoted by a thick solid line, while its dual of strength $\widetilde{K}$ is denoted by a thick dashed line.

specific realization of a RBAT on a square lattice with couplings (K^1, Λ^1), (K^2, Λ^2) distributed at random with probabilities p and $1 - p$, respectively. Replacing each bond by its dual we obtain (on the dual lattice) a system with couplings $(\widetilde{K^1}, \widetilde{\Lambda^1})$ and $(\widetilde{K^2}, \widetilde{\Lambda^2})$, distributed at random with probabilities p and $1 - p$. This defines a one to one mapping under duality from the ensemble of realizations of $[(K^1, \Lambda^1), (K^2, \Lambda^2), p]$ RBAT systems, onto the ensemble of the dual systems $[(\widetilde{K^1}, \widetilde{\Lambda^1}), (\widetilde{K^2}, \widetilde{\Lambda^2}), p]$. Under duality each bond is mapped onto the bond on the dual lattice which intersects the original bond (see Fig. 1). Thus the spatial distribution of the two types of bonds on the dual lattice is different from that of the original lattice. However, since all spatial distributions have the same weight in their ensemble, there is a one to one correspondence of bond configurations in the two ensembles, and we can write

$$f_s[(K^1, \Lambda^1), (K^2, \Lambda^2), p] = f_s[(\widetilde{K^1}, \widetilde{\Lambda^1}), (\widetilde{K^2}, \widetilde{\Lambda^2}), p] ,$$

$$\text{(9)}$$

where it is understood that in calculating f_s we average over all spatial bond distributions. Choosing $p = \frac{1}{2}$ we find that there is a self-dual manifold at $(K^2, \Lambda^2) = (\widetilde{K^1}, \widetilde{\Lambda^1})$. Our ability to locate a self-dual manifold for the case $p = \frac{1}{2}$ makes this choice of p a convenient case for studying the RBAT. Viewing the duality transformation as a mathematical mapping in the space of couplings $[(K^1, \Lambda^1), (K^2, \Lambda^2), \frac{1}{2}]$, it is identical to the duality transformation in the space of couplings $[(K^1, \Lambda^1), (K^2, \Lambda^2)]$ of the anisotropic AT model. Thus all conclusions which were based on duality in Sec. II A apply here equally. Following the logic of Sec. II A, we conjecture that the subspace of the RBAT for which $0 \leq \Lambda^1 \leq K^1$, $0 \leq \Lambda^2 \leq K^2$ and $p = \frac{1}{2}$ includes in it a critical plane defined by $0 \leq \Lambda^1 \leq K^1$, $(K^2, \Lambda^2) = (\widetilde{K^1}, \widetilde{\Lambda^1})$.

In order to study the effect of randomness on the AT model we need a reference nondisordered system for comparison. When studying a specific RBAT model with couplings $[(K^1, \Lambda^1), (K^2, \Lambda^2), \frac{1}{2}]$ it is not clear with which specific nonrandom AT model with couplings (K, Λ) one should compare. Nonetheless a comparison with the corresponding AAT model with couplings $[(K^1, \Lambda^1), (K^2, \Lambda^2)]$ seems to be quite natural. Consider the anisotropic model with bonds (K^1, Λ^1) in the horizontal direction and bonds (K^2, Λ^2) in the vertical direction. Next, consider as a perturbation, a change of a small fraction p of the bonds in the horizontal direction into bonds of strength (K^2, Λ^2) and the same fraction of bonds in the vertical direction into bonds of strength (K^1, Λ^1). When p increases all the way to $p = \frac{1}{2}$ the anisotropy disappears and the model is completely random. So, in a sense, the perturbation of randomness can take us continuously from the critical plane of the anisotropic model to the critical plane of the random model. In view of this simple picture we have performed simulations of the anisotropic and random-bond AT models at several points on their self-dual planes described above. We indeed find the two planes to be critical. In Sec. III we give some details of the simulations.

III. METHOD AND DETAILS OF SIMULATIONS

A. The method

In Ref. [22] we described a cluster algorithm for the AT model and tested its performance (on the isotropic model). As explained there, the algorithm can be regarded from two different points of view. The conceptually simpler and faster (though less general) one is that of the Wolff embedding idea [36,37]. It is faster in the sense that its implementation on the computer runs faster since the freeze-delete procedure is less complicated. The main idea is to embed into the AT model an Ising model of space dependent couplings J_{jk} and simulate it using the SW [38] or Wolff [36] procedures for the Ising model. To be explicit, consider the Hamiltonian (5), and take the τ variables as fixed, so we can write

$$\mathcal{H} = \mathcal{H}_1 + \mathcal{H}_2 = -\sum_{\langle i,j \rangle} (K_{i,j} + \Lambda_{i,j} \tau_i \tau_j) \sigma_i \sigma_j$$
$$- \sum_{\langle i,j \rangle} K_{i,j} \tau_i \tau_j. \qquad \text{(10)}$$

$\mathcal{H}_2$ represented by the second sum is a constant, and remembering that we are considering $\Lambda_{i,j} \leq K_{i,j}$ for all (i,j), $\mathcal{H}_1$ is a ferromagnetic Ising model in the σ variables with couplings $J_{i,j} = K_{i,j} + \Lambda_{i,j} \tau_i \tau_j$. Simulating this Ising model with any procedure that will maintain detailed balance with respect to $\mathcal{H}_1$ and will not change the value of $\mathcal{H}_2$, will also maintain detailed balance with respect to $\mathcal{H}$. So we can use, for example, the SW [38] or Wolff [36] procedures for the Ising model. This by itself will maintain detailed balance but will not be ergodic since the τ variables will not be updated. Obviously, to update the τ variables the same process should be repeated, holding the σ variables fixed and simulating an Ising Hamiltonian with the τ variables. To summarize, our procedure goes as follows: Choose at random whether to embed into the AT Hamiltonian an Ising Hamiltonian in the σ (or τ) spins. Pick a random site in the lattice, grow a cluster of σ (or τ) spins, using the Wolff single cluster procedure with the Ising Hamiltonian [(10) or the opposite one in case of a τ embedding], and flip it.

B. Choice of simulation points

All our simulations were performed at the critical plane defined by

$$\{[(K^1, \Lambda^1), (K^2, \Lambda^2), p = \tfrac{1}{2}] : (K^2, \Lambda^2) = (\widetilde{K^1}, \widetilde{\Lambda^1}),$$
$$0 \leq \Lambda^1 \leq K^1 \} , \quad \text{(11)}$$

as explained in Sec. II (for the anisotropic model just omit the $p = \frac{1}{2}$). For convenience we also use the following notation for the coupling constants:

$$Z = \exp(-4K), X = \exp[-2(K + \Lambda)],$$
$$\vec{X} = (X, Z) . \qquad \text{(12)}$$

The first series of measurements were performed at five points $(\vec{X^1}_i, \vec{X^2}_i)$, $i = 0, \ldots, 4$, which we label as C_i, $i = 0, \ldots, 4$. These were chosen so as to interpolate between $(\vec{X^1_0}, \vec{X^2_0})$, which is an anisotropic (or random-bond) decoupled Ising critical point, and $(\vec{X^1_4}, \vec{X^2_4})$, which is an anisotropic (or random-bond) four-state Potts critical point. The points C_i interpolate in a similar manner to the way in which the critical line of the pure AT connects the pure decoupled Ising critical point with the pure four-state Potts critical point. Thus we chose the five points $\vec{X^1_i}$ to lie equidistantly on the line

$$Z^1 - Z^1_{\text{Ising}} = -2(X^1 - X^1_{\text{Ising}}) \ . \tag{13}$$

The slope -2 was chosen so that line (13) lies parallel (in the XZ plane) to the critical line of the pure AT model, $Z = 1 - 2X$. Note that once (X^1, Z^1) are defined, (X^2, Z^2) are defined through (11) and (12).

We clearly have some freedom in our choice of $(X^1_{\text{Ising}}, Z^1_{\text{Ising}})$, the decoupled Ising couplings; setting $\Lambda^1 = 0$ in (11) one obtains $\Lambda^2 = \widetilde{\Lambda^1} = 0$ as well. The remaining parameter K^1 is chosen so that [see (11)]

$$K^2_{\text{Ising}} = \widetilde{K^1_{\text{Ising}}} = \frac{1}{10} K^1_{\text{Ising}}. \tag{14}$$

Since the extent of deviation from pure behavior is obviously determined not only by p but also by the difference between the two sets of couplings, the ratio of $\frac{1}{10}$ was chosen so that randomness will be pronounced [32,39].

While (14) defines the first simulation point $\vec{X^1_0} \equiv \vec{X^1_{\text{Ising}}}$, the fifth simulation point $\vec{X^1_4} \equiv \vec{X^1}_{\text{Potts}}$ is chosen to be a four-state Potts point lying at the intersection of line (13) with the four-state Potts line $Z^1 = X^1$ (or $\Lambda^1 = K^1$).

The other three simulation points $\vec{X^1_{1,2,3}}$ lie equidistantly on the line (13) between $\vec{X^1_{\text{Ising}}}$ and $\vec{X^1_{\text{Potts}}}$:

$$X^1_i = \frac{i}{4}(X^1_{\text{Potts}} - X^1_{\text{Ising}}) + X^1_{\text{Ising}},$$
$$Z^1_i = Z^1_{\text{Ising}} - 2(X^1_i - X^1_{\text{Ising}}) \quad i = 0, \ldots, 4 \ , \tag{15}$$

Thus the first series of points C_i at which we made measurements $C_{0,\ldots,4}$ is defined through Eqs. (11), (12), (14), and (15) and the definition of $\vec{X^1_{\text{Potts}}}$.

Two additional measurement points were intended to monitor the effect of varying the amount of randomness in the model on the critical behaviour. In order to define these two points we define two series of five points each, $A_{0\ldots4}$ and $B_{0\ldots4}$. Similarly to the series $C_{0\ldots4}$, these two series are defined through Eqs. (11), (12), and (15). But in contrast with the series $C_{0,\ldots,4}$, Eq. (14) is substituted with

$$\frac{K^2_{\text{Ising}}}{K^1_{\text{Ising}}} = \frac{1}{2} \tag{16}$$

for the series $A_{0\ldots4}$, and with

$$\frac{K^2_{\text{Ising}}}{K^1_{\text{Ising}}} = \frac{1}{4}. \tag{17}$$

for the series $B_{0\ldots4}$. Though we defined here ten additional points we actually performed measurements only at the points A_2 and B_2. The points A_2, B_2, and C_2 represent three RBAT (or AAT) models with coupling ratios $\frac{\Lambda^1}{K^1} \approx \frac{1}{2}$ and $\frac{K^2}{K^1} \approx \frac{1}{2}$, $\frac{1}{4}$, and $\frac{1}{10}$ respectively.

C. MC simulations

We calculated the energy [40] per site:

$$E = [\langle E \rangle] = -\frac{1}{L^2}\left[\left\langle \sum_{\langle i,j \rangle}\{K_{i,j}(\sigma_i\sigma_j + \tau_i\tau_j) \right.\right.$$
$$\left.\left. + \Lambda_{i,j}\sigma_i\tau_i\sigma_j\tau_j\} \right\rangle\right] \tag{18}$$

where L is the linear lattice size, and the angular brackets denote the usual thermal MC average, whereas the square brackets denote the quenched average over random-bond configurations. The specific heat per site follows from the energy fluctuations

$$C = \frac{C_h}{k_B} = L^2[\langle E^2 \rangle - \langle E \rangle^2]. \tag{19}$$

We define

$$m_\sigma = \frac{1}{L^2}\sum_i \sigma_i, \quad m_\tau = \frac{1}{L^2}\sum_i \tau_i, \quad m_{\sigma\tau} = \frac{1}{L^2}\sum_i \sigma_i\tau. \tag{20}$$

To compute the magnetization per site, M, we used

$$M = \frac{1}{2}[\langle |m_\sigma| + |m_\tau| \rangle], \tag{21}$$

taking advantage of the symmetry between the σ and τ spins to increase accuracy. Another order parameter of the transition plane we are considering is the polarization [23] P, defined as

$$P = [\langle |m_{\sigma\tau}| \rangle], \tag{22}$$

which measures the magnetization of the $\sigma\tau$ spins. We calculated the magnetic susceptibility of the σ spins using [40]

$$\chi = \frac{L^2}{2}[\langle m_\sigma^2 + m_\tau^2 \rangle] \tag{23}$$

and also measured c, the size of the cluster flipped at each step, and calculated $\langle c \rangle$. There is a connection between the size of the clusters and the susceptibility [41] which is common for all algorithms that generate noninteracting clusters of spins (if all spins in a cluster have the same value). For the Wolff single cluster procedure it has the simple form [36]

$$\chi = \langle c \rangle. \tag{24}$$

Finally we measured the susceptibility of the $\sigma\tau$ spins, χ_p:

$$\chi_P = L^2[\langle m_{\sigma\tau}^2\rangle]. \qquad (25)$$

For each sample we estimated the effective autocorrelation times [42] of the energy, τ_E^{eff} and the magnetization τ_M^{eff} using the method outlined in Ref. [36]. The length of an individual run was often too short for a precise estimate, but averaging over all samples gave a rough estimate of $[\tau_{E,M}^{\text{eff}}]$. These estimates of τ^{eff} allowed us to verify that all samples were equilibrated well enough before we started collecting data. Typically we discarded at least $50\tau_E^{\text{eff}}$ spin configurations.

The fluctuations in the random-bond configurations introduce, in addition to the usual MC error, another source of statistical error. Thus the total error for the specific heat, δC, for example, is given by

$$(\delta C)^2 = \frac{\sigma_n^2}{n} + \frac{\sigma_T^2}{nT_{MC}/\tau}, \qquad n, T_{MC} \ \text{large}, \quad (26)$$

where n is the number of random-bond samples, T_{MC} is the length of the MC runs and τ is the autocorrelation time of the algorithm (which we can estimate by τ^{eff}). σ_T^2 is the variance of C within a given sample and is due to thermal fluctuations, while σ_n^2 is the variance of the exact $\langle C\rangle$ within the ensemble of random-bond samples. Thus both the thermal fluctuations and sample to sample fluctuations contribute to the error.

We found that both terms in (26) imply that simulations of the AT models and the Potts model are much more expensive in computer time than simulations of the Ising model. First there is an increase in τ in consistence with our findings in the pure models [22]. That is, at $L = 256$ for the random Ising model we find $\tau_E^{\text{eff}} \approx 3.1(1)$ compared with $\tau_E^{\text{eff}} \approx 11.3(3)$ for the random four-state Potts model. Second we found that for all thermodynamic quantities P the relative variance σ_n^2/P^2 was larger for the random four-state Potts model than for the random Ising model. This effect was strongest for the specific heat, e.g., for $L = 256$, $\sigma_{n,C}^2/C^2$ of the random four-state Potts model was approximately an order of magnitude larger than that of the random Ising model. In accordance with these findings, the number of samples simulated for the Ising model varied between $n = 1000$ for $L = 4$ and $n = 150$ for $L = 256$, while for the four-state Potts model it varied between $n = 2000$ for $L = 4$ and $n = 330$ for $L = 256$.

IV. MONTE CARLO RESULTS

A. Specific heat

We expect the critical specific heat of the AAT to follow the finite size scaling [43] form of (3),

$$C \approx a_1 + b_1 L^{\alpha/\nu}. \qquad (27)$$

The exponent ratio $\frac{\alpha}{\nu}$ is predicted analytically [23,24] to

vary continuously along the critical line of the pure AT model between $\frac{\alpha}{\nu} = 0$ at the decoupled Ising critical point and $\frac{\alpha}{\nu} = 1$ at the four-state Potts critical point. One expects the same variation to hold for the corresponding critical manifold of the AAT at which the simulations were performed. In Fig. 2 we plot the critical specific heat C as a function of $\ln L$ for the five critical AAT models $C_{0,..,4}$. Fits are made to form (27), and the estimated values of α/ν are listed in Table I. Since model C_0 is an anisotropic Ising model, its specific heat does not follow form (27), but rather $C \approx A + B\ln L$. The anisotropic four-state Potts model C_4 should have $\alpha/\nu = 1$ with a logarithmic correction [44] to scaling $C \sim L/\ln^{3/2} L$. In the range of L considered, the logarithmic correction results in an estimate for α/ν which is too low. The results for the specific heat of the AAT models clearly demonstrate a variation of α/ν from its Ising value ($\alpha/\nu = 0$), to its four state Potts value. As will be seen shortly this is quite different from the results for the RBAT models.

In order to analyze the specific-heat results of the RBAT we first tried to fit the results to (27), but unlike the specific heat of the AAT this was not possible for the full lattice size range $4 \leq L \leq 256$. Thus in Fig. 3 we show the specific heat as a function of $\ln L$ for the five critical RBAT models $C_{0,..,4}$ along with fitting curves to (27), where only data for $L \geq 24$ were used to fit. The estimated exponents α/ν obtained from these fits are 0 within errors, indicating a possible logarithmic behavior. In addition, Fig. 3 indicates a crossover of the effective exponents (the slope between every two successive data points) from higher to lower values. Physically we expect that this is due to a crossover from the pure models' exponents to some alternative random critical behavior. We are thus led to the following finite size scaling ansatz for the specific heat

$$C = a_0 + b_0 \ln[1 + c_0(L^{(\alpha/\nu)_p} - 1)], \qquad (28)$$

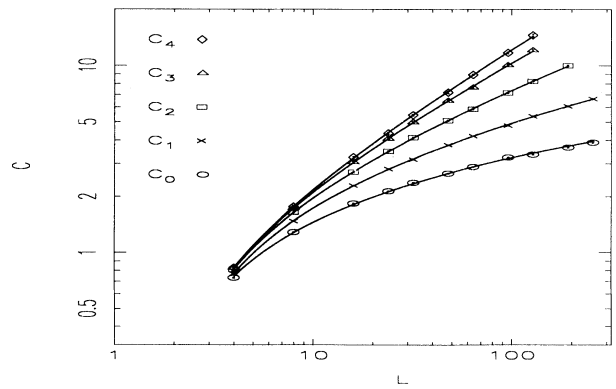where $(\alpha/\nu)_p$ is the critical exponent ratio of the cor-

FIG. 2. Specific heat C as a function of $\ln L$ for five critical models $C_{0,..,4}$, of the AAT. Note that C_0 is an anisotropic decoupled Ising model and C_4 is an anisotropic four-state Potts model. The curves are fits to (27), yielding estimates for $\frac{\alpha}{\nu}$ which are listed in Table I.

TABLE I. Critical exponents ratios and fitting parameters from the first series of simulations $C_{0,...,4}$ and the second series $A, B,$ and C_2 of the Anisotropic AT model. The exponent ratios and parameters are defined in the text.

	$\frac{\alpha}{\nu}$	$\frac{\gamma}{\nu}$	$\frac{\beta}{\nu}$	$\frac{\gamma_p}{\nu}$	$\frac{\beta_p}{\nu}$
C_0	0.0001(150)	1.7511(7)	0.1244(4)	1.501(1)	0.2494(6)
C_1	0.171(5)	1.751(1)	0.1242(5)	1.554(1)	0.2231(5)
C_2	0.375(5)	1.755(1)	0.1223(7)	1.608(2)	0.197(1)
C_3	0.549(8)	1.759(4)	0.1199(27)	1.667(5)	0.169(3)
C_4	0.630(8)	1.749(4)	0.1238(21)	1.750(4)	0.1237(26)
B_2	0.371(5)	1.753(1)	0.1233(7)	1.608(2)	0.197(1)
A_2	0.40(1)	1.750(1)	0.1254(8)	1.603(2)	0.199(1)

responding pure model and $c_0 = \frac{g}{(\alpha/\nu)_p}$. An important point to note is that for each random-bond AT model, following the discussion at the end of Sec. II B, $(\alpha/\nu)_p$ is taken from our results (listed in Table I) for the corresponding anisotropic AT model. g is a measure of the randomness, and is related through the relation

$$c_0 = (L_c^{(\alpha/\nu)_p} - 1)^{-1} , \qquad (29)$$

to a crossover length L_c, at which crossover from the pure model's power law behavior to the random logarithmic behavior occurs. Thus for $L \ll L_c$ our Eq. (28) reduces to (27) while for $L \gg L_c$ and $L_p^{(\alpha/\nu)} \gg 1$ a logarithmic behavior is attained:

$$C = a + b \ln L . \qquad (30)$$

Apart from crossing over to the correct pure result (27) when $c_0 \to 0$, Eq. (28) was constructed so that in the Ising model limit, $(\alpha/\nu)_p \to 0$ it becomes

$$C = a + b \ln(1 + g \ln L) . \qquad (31)$$

This is the finite size scaling form of (1) which was shown by Wang et al. [32] to fit the random-bond Ising model well. This form will be examined below as another can-
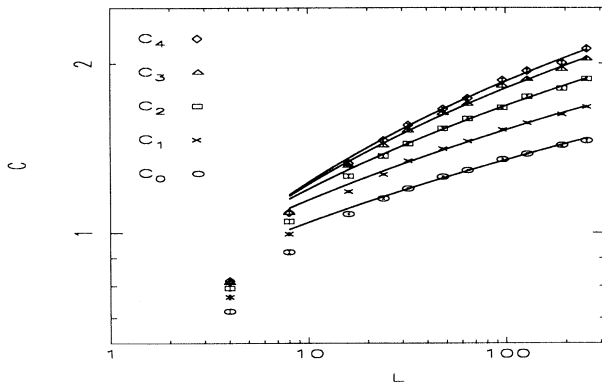
didate for describing the RBAT models.

In Fig. 4 the specific heat of the five critical RBAT models $C_{0,...,4}$ are plotted again but with fits to (28) using the full lattice size range $4 \leq L \leq 256$, on a semilogarithmic scale. The fitting parameters are listed in Table II. For these points (with large randomness $\frac{K^2}{K^1} \approx \frac{1}{10}$), the crossover lengths L_c are found to be 1.

In Fig. 5 the specific heats of three critical RBAT models $A_2, B_2,$ and C_2 are plotted with the fitting functions of (28). $(\alpha/\nu)_p$ is taken from the corresponding anisotropic models and the fitting parameters are listed in Table II. $(\alpha/\nu)_p$ of the three models $A_2, B_2,$ and C_2 is very similar (0.40, 0.37, 0.37, respectively), but they differ in their amount of randomness, $\frac{K^2}{K^1} \approx \frac{1}{2}, \frac{1}{4},$ and $\frac{1}{10}$ respectively. Form (28) seems to describe all three models adequately with the main change being in the crossover length L_c which decreases as randomness increases. The estimates for L_c can be compared with results from random-bond Ising models [10,32] with the same coupling ratios. For $\frac{K^2}{K^1} \approx \frac{1}{10}, \frac{1}{4},$ and $\frac{1}{2}$ we obtain $L_c = 1, 4. \pm .04,$ and $L_c = 51 \pm 7$ compared with $L_c = 2 \pm 1$, $L_c = 16 \pm 4$, and $L_c \sim 1000$ for the respective Ising models. According to the Harris criterion, one expects the crossover length to scale roughly as

$$L_c \sim R^{-\frac{1}{\phi}} , \qquad (32)$$

where $\phi = (\alpha/\nu)_p$ is the crossover exponent and R ($R < 1$, $R \sim \frac{K^1}{K^2}$) is a measure of the randomness. For the RBAT models considered here $(\alpha/\nu)_p \approx 0.37$, while for the random-bond Ising models randomness is marginal $[(\alpha/\nu)_p = 0]$, so that the much smaller crossover lengths that we find are consistent with the Harris criterion.

Since there is no theoretical prediction for the critical behavior of the RBAT model, we examined possible scaling forms for the specific heat other than (28). A natural candidate is a double logarithmic behavior as in Eq. (1). This form was predicted by DD for the disordered Baxter [27] and Ising [10,32] models, and confirmed for the latter model. In its asymptotic limit, the finite size scaling form of (1) is
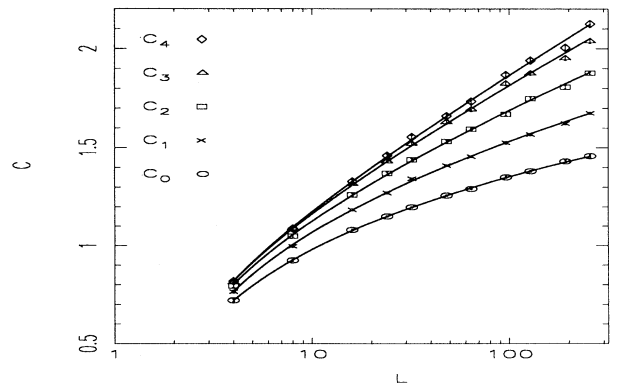

FIG. 3. Specific heat C as a function of $\ln L$ for five critical models $C_{0,..,4}$, of the RBAT. Note that C_0 is a random-bond decoupled Ising model, and C_4 is a random-bond four-state Potts model. The curves are fits to form (27) for lattice sizes $L \geq 24$.

FIG. 4. Specific heat C as a function of $\ln L$ for five critical models $C_{0,..,4}$, of the RBAT. The curves are fits to form (28), yielding estimates for the coefficients of (28) which are listed in Table II.

TABLE II. Fitting parameters for the fits in Figs. 4 and 5 according to Eqs. (28) and (29). Errors are given in parentheses only when the error is smaller than or of the same order as the number itself.

	a_0	b_0	c_0	L_c
C_0	-0.37(12)	0.58(1)	5.2E4(1.5E4)	1.0
C_1	-4.6	0.51(2)	1.5E6	1.0
C_2	-4.1	0.46(127)	5.5E4	1.0
C_3	-3.9	0.43(4)	5.5E4	1.0
C_4	-4.1	0.42(1)	1.0E5	1.0
B_2	-0.09(5)	2.00(4)	1.47(10)	4.0(4)
A_2	-0.07(6)	9.35(33)	0.26(2)	51(7)

$$C = a + b \ln \ln L . \tag{33}$$

We compare this form with (30) as both these forms are asymptotic and do not include crossover from the pure behavior. In Fig. 6 we again plot our specific-heat results for all the models tested except for A_2, which is not considered due to its large crossover length. The results are fitted by (30) in Fig. 6 and by (33) in Fig. 7, for $L \geq 16$.

As found by Wang et al., for the random-bond Ising model C_0, agreement with (33) is much better than with (30), according to our error analysis. For model C_1, agreement with (33) is also better, but this can be attributed to slow crossover behavior from the small power law $(\alpha/\nu)_p \approx 0.17$ [the condition $L_p^{(\alpha/\nu)} \gg 1$ is not fulfilled for such small $(\alpha/\nu)_p$ and for the range of L considered]. For models $C_{2,3}$ the quality of both fits is comparable while for the random-bond four-state Potts C_4 the fit (30) is better. For model B_2 we obtained larger statistics (more than 900 samples for $L \leq 128$ and 300 samples for $L = 256$), and the result is conclusively in favor of (30).

Last we considered the possibility that the crossover from power law behavior to logarithmic behavior is followed at even larger L by a crossover to a double logarithmic behavior. This was done by fitting the specific-heat data for $L \geq 16$ according to (31). Though the
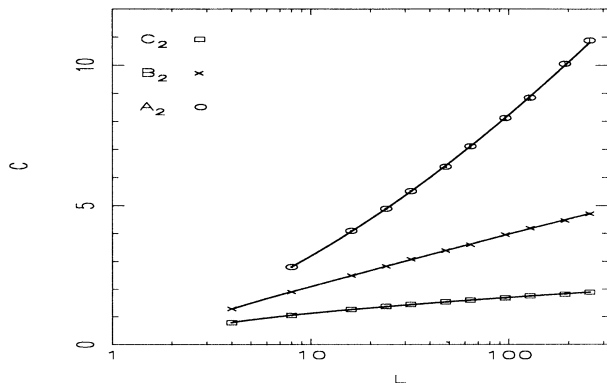

FIG. 6. Specific heat C as a function of $\ln L$ for the RBAT critical models B_2 and $C_{0,...,4}$ with fitting curves of (30).

fits were of good quality, the estimated crossover lengths $L_i = \exp(1/g)$ did not make sense physically. For the B_2 model we found $L_i > 10^8$, which actually implies a logarithmic behavior for all accessible values of L. This should be compared with our estimate $L_c \approx 4$ and the value $L_i \approx 16$ for the corresponding Ising model (see above). For models $C_{0,...,4}$ we find that L_i increases monotonically from the Ising model C_0 where $L_i \approx 2$, to the four-state Potts model C_4 where $L_i \approx 200$. This is contrary to the expectation that the crossover length should decrease due to the increase in the crossover exponent $\phi = (\alpha/\nu)_p$, as implied in (32).

We conclude that our results are in favor of a logarithmic divergence of the specific heat and not a double logarithmic one for the RBAT model, excluding the random-bond Ising model. The finite size scaling form (28) gives the best agreement with our results for all models, including those with weak randomness, and for the full lattice size range $4 \leq L \leq 256$. Thus for $C(t)$ we predict the scaling form

$$C \sim \ln[1 + b(t^{-\alpha_p} - 1)], \tag{34}$$

A possibility which we tend to rule out is that both types

FIG. 5. Specific heat C as a function of $\ln L$ for three critical models A_2, B_2, C_2, of the random bond AT. The curves are fits to form (28), yielding estimates for the coefficients of (28) which are listed in Table II.
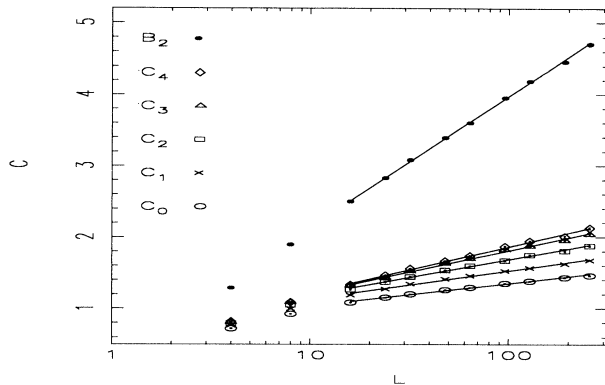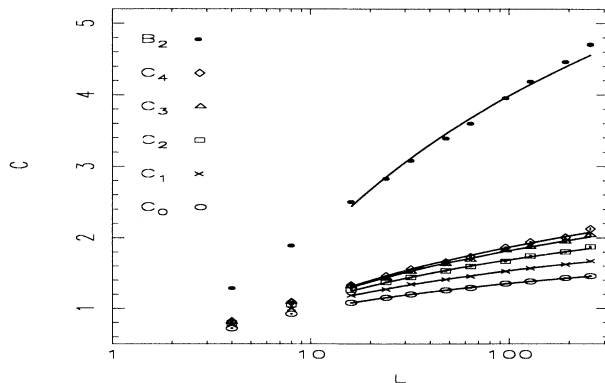

FIG. 7. Specific heat C as a function of $\ln L$ for the RBAT critical models B_2 and $C_{0,...,4}$ with fitting curves of (33).

of critical behaviors [that is, (34) and (1)] occur, and that there is some bifurcation plane which separates the two types of behaviors.

B. Susceptibility and magnetization

1. Susceptibility

According to finite size scaling theory one expects that the critical susceptibility diverges as

$$\chi \sim L^{\frac{\gamma}{\nu}} \tag{35}$$

for large enough L. The exponents' ratio γ/ν is predicted analytically [23,24] to be constant, $\gamma/\nu = \frac{7}{4}$, all along the critical line of the pure AT model. This is expected also to hold for the corresponding critical manifold of the AAT. Figure 8 shows results for the critical susceptibility as a function of $\ln L$ for the five critical models, $C_{0,..,4}$, of the AAT. So that the points do not fall on top of each other, χ for the model C_i has been multiplied by 2^i. The solid lines are linear fits to form (35) for $L \geq 24$, yielding estimates for critical exponents $\frac{\gamma}{\nu}$ which are listed in Table I. All results seem to be consistent with the analytic prediction, giving a combined best estimate of $\gamma/\nu = 1.7512(6)$. An effective exponent analysis (or a trend analysis) shows that, as $\ln L$ increases, $(\frac{\gamma}{\nu})_{\rm eff}$ approaches the value $\frac{7}{4}$ from above.

The finite size scaling form (35) and the value of $\frac{\gamma}{\nu} = \frac{7}{4}$ have been predicted [7–9] for the disordered decoupled Ising model and confirmed in MC simulations [10,32]. Figure 9 shows results for the critical susceptibility as a function of $\ln L$ for the five random critical models $C_{0,..,4}$, of the RBAT. The same analysis has been carried out as for the AAT, and the estimated critical exponents $\frac{\gamma}{\nu}$ are listed in Table III. The estimates for the decoupled Ising critical point C_0 and for models $C_{1,2}$ are consistent with $\frac{\gamma}{\nu} = \frac{7}{4}$. On the other hand for the model C_3 and
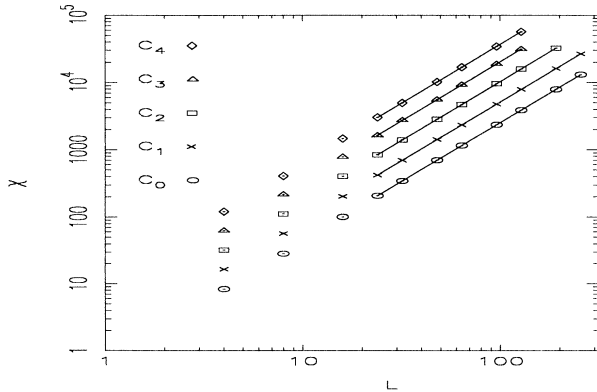

FIG. 9. Susceptibility as a function of $\ln L$ for five critical models $C_{0,..,4}$ of the RBAT. For the sake of clarity χ for model C_i has been multiplied by 2^i. The solid lines are linear fits to form (35) for $L \geq 24$, yielding estimates for critical exponents $\frac{\gamma}{\nu}$ which are listed in Table III.
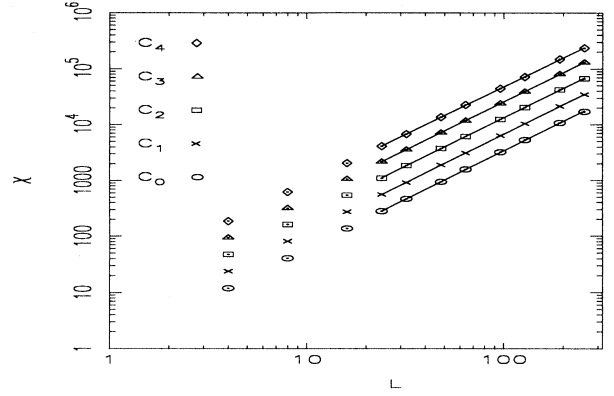
the random-bond four-state Potts model C_4 we obtain $\frac{\gamma}{\nu} = 1.736(3)$ and $\frac{\gamma}{\nu} = 1.714(5)$ respectively. We also tried fitting the results with the form

$$\chi = A_\chi L^{\frac{7}{4}} (\ln L)^{-p_\chi} , \tag{36}$$

for $L \geq 24$. The obtained estimate for p_χ is listed in Table III. for the random-bond four state Potts model we find $p_\chi = 0.148(21)$ while for the models C_{0-2} the error in p_χ is at least of the same order as the estimate for p_χ itself.

2. Magnetization

The critical magnetization of the five anisotropic models is expected [23,24] to follow the form

$$M \sim L^{-\frac{\beta}{\nu}} , \tag{37}$$

with $\frac{\beta}{\nu} = \frac{1}{8}$. Applying straightforward finite size scaling analysis, as described above for the susceptibility, to the magnetization results, we obtained estimates for $\frac{\beta}{\nu}$

FIG. 8. Susceptibility as a function of $\ln L$ for five critical models $C_{0,..,4}$ of the AAT. For the sake of clarity, χ for model C_i has been multiplied by 2^i. The solid lines are linear fits to form (35) for $L \geq 24$, yielding estimates for critical exponents $\frac{\gamma}{\nu}$ which are listed in Table I.

TABLE III. Critical exponents ratios and fitting parameters from the first series of simulations $C_{0,..,4}$ and the second series $A, B,$ and C_2 of the random-bond AT. These exponents and parameters related to the scaling of the order parameters are defined in the text.

	$\frac{\gamma}{\nu}$	p_χ	$\frac{\beta}{\nu}$	p_m	$\frac{\gamma_p}{\nu}$	$\frac{\beta_p}{\nu}$
C_0	1.751(5)	-0.007(20)	0.125(3)	-0.003(12)	1.549(9)	0.227(5)
C_1	1.751(6)	-0.008(19)	0.124(3)	-0.004(11)	1.575(8)	0.214(5)
C_2	1.743(5)	0.026(22)	0.129(3)	0.015(14)	1.597(9)	0.205(5)
C_3	1.736(3)	0.057(14)	0.133(2)	0.032(9)	1.638(5)	0.185(3)
C_4	1.714(5)	0.148(21)	0.145(3)	0.082(13)	1.714(5)	0.145(3)
B_2	1.738(4)	-0.049(17)	0.132(3)	0.029(10)	1.586(6)	0.209(4)
A_2	1.739(5)	-0.042(22)	0.132(3)	0.027(13)	1.590(8)	0.208(5)

which are listed in Table I. The results are slightly below the expected value, but an effective exponent analysis (or a trend analysis) shows that as $\ln L$ increases $(\frac{\beta}{\nu})_{\text{eff}}$ approaches the value $\frac{1}{8}$ from below.

The finite size scaling form (37) and the value of $\frac{\beta}{\nu} = \frac{1}{8}$ have been predicted [7–9] for the disordered decoupled Ising model and confirmed in MC simulations [10,32]. Figure 10 shows results for the critical magnetization as a function of $\ln L$ for the five critical models, $C_{0,..,4}$, of the RBAT. A fit to form (37) yields the estimated critical exponents $\frac{\beta}{\nu}$ listed in Table III. The estimates for the decoupled Ising critical point C_0 and for models $C_{1,2}$ are consistent with $\frac{\beta}{\nu} = \frac{1}{8}$. On the other hand for the model C_3 and the random-bond four-state Potts model C_4 we obtain $\frac{\beta}{\nu} = 0.133(2)$ and $\frac{\beta}{\nu} = 0.145(3)$ respectively. We also tried fitting the results with the form

$$M = A_m L^{-\frac{1}{8}} (\ln L)^{-p_m} , \qquad (38)$$

for $L \geq 24$. The obtained estimate for p_m is listed in Table III. For the random-bond four-state Potts model we find $p_m = 0.082(13)$ while for models C_{0-2} the error in p_1 is at least of the same order as the estimate for p_m itself.

3. Polarization and χ_p

Since the polarization is an order parameter of the transition, the critical polarization P and χ_p should follow the forms:

$$P \sim L^{\frac{-\beta_p}{\nu}} , \qquad (39a)$$

$$\chi_p \sim L^{\frac{\gamma_p}{\nu}} . \qquad (39b)$$

The critical exponents ν, β_p, and γ_p are known analytically [23,24] all along the critical line of the pure AT
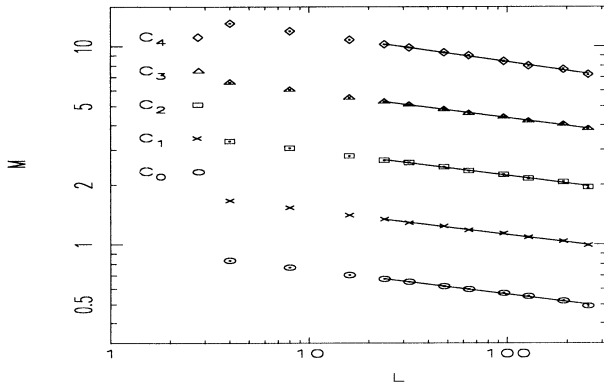
model. For example, the ratio $\frac{\beta_p}{\nu}$ varies continuously between its value at the decoupled Ising critical point, $\frac{\beta_p}{\nu} = \frac{1}{4}$, and its value at the four-state Potts critical point, $\frac{\beta_p}{\nu} = \frac{1}{8}$. These two extreme values can be obtained, through their relations with $\frac{\beta}{\nu}$, for any (pure, anisotropic or disordered) decoupled Ising or four-state Potts model. For the decoupled Ising models $\Lambda^1 = \Lambda^2 = 0$ (or $\Lambda = 0$ for the pure model), the σ spins system and the τ spins system are decoupled, hence

$$P = \langle \sigma\tau \rangle = \langle \sigma \rangle\langle \tau \rangle = M^2 \sim t^{2\beta} . \qquad (40)$$

This implies $\beta_p = 2\beta$ for all the decoupled Ising models. For the four-state Potts models $K^1 = \Lambda^1$ and $K^2 = \Lambda^2$ (or $K = \Lambda$ for the pure four-state Potts) so that σ spins, τ spins and $\sigma\tau$ spins are equivalent, and

$$P = \langle \sigma\tau \rangle = \langle \sigma \rangle = \langle \tau \rangle = M . \qquad (41)$$

It follows that $\beta_p = \beta$. Thus interpreting our results as $\frac{\beta}{\nu} = \frac{1}{8}$ for the critical plane of the RBAT implies $\frac{\beta_p}{\nu} = 2\frac{\beta}{\nu} = \frac{1}{4}$ for the random-bond decoupled Ising model, and $\frac{\beta_p}{\nu} = \frac{\beta}{\nu} = \frac{1}{8}$ for the random-bond four-state Potts model. The question still remains whether the variation between these two values along the critical plane of the RBAT will be continuous, as is the case for the pure model, or whether it will become discontinuous under the influence of disorder. The results presented below are in favor of a continuous variation. The values of $\frac{\gamma_p}{\nu}$ can be obtained through the scaling relation,

$$2\frac{\beta_p}{\nu} + \frac{\gamma_p}{\nu} = d , \qquad (42)$$

which our results fully confirm. This leads to $\frac{\gamma_p}{\nu} = \frac{3}{2}$ for the Ising models and $\frac{\gamma_p}{\nu} = \frac{7}{4}$ for the four-state Potts models.

Figures 11 and 12 show the critical χ_p and polarization, P, respectively, as a function of $\ln L$ for the five critical models, $C_{0,..,4}$, of the AAT. The solid lines are linear fits

FIG. 10. Magnetization as a function of $\ln L$ for five critical models $C_{0,..,4}$ of the RBAT. For the sake of clarity M for model C_i has been multiplied by 2^i. The solid lines are linear fits to form (37) for $L \geq 24$, yielding estimates for critical exponents $\frac{\beta}{\nu}$ which are listed in table III.
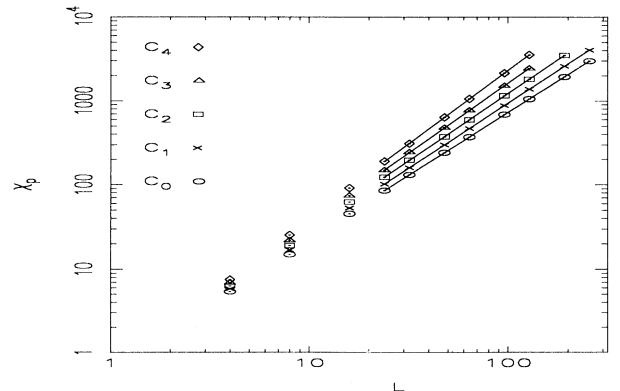

FIG. 11. χ_p as a function of $\ln L$ for five critical models $C_{0,..,4}$, of the AAT. The solid lines are linear fits to the form 39b) for $L \geq 24$, yielding estimates for critical exponents $\frac{\gamma_p}{\nu}$ which are listed in Table I.
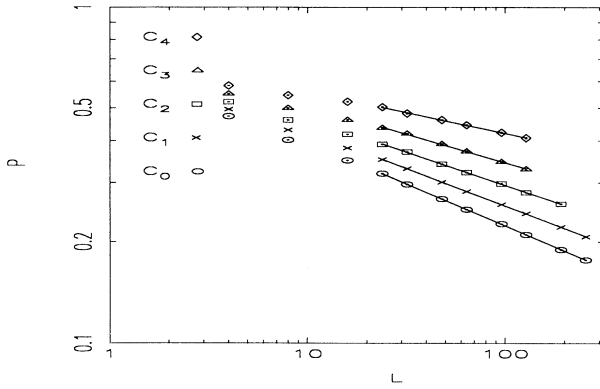
FIG. 12. Polarization P as a function of $\ln L$ for five critical models $C_{0,...,4}$ of the AAT. The solid lines are linear fits to the form (39a) for $L \geq 24$, yielding estimates for critical exponents $\frac{\beta_p}{\nu}$ which are listed in Table I.

FIG. 14. Polarization P as a function of $\ln L$ for five critical models, $C_{0,...,4}$, of the RBAT. The solid lines are linear fits to form (39a) for $L \geq 24$, yielding estimates for critical exponents $\frac{\beta_p}{\nu}$ which are listed in Table IV.

to forms (39) for $L \geq 24$, yielding estimates for critical exponents $\frac{\gamma_p}{\nu}$ and $\frac{\beta_p}{\nu}$ which are listed in Table I. As expected, we find that $\frac{\gamma_p}{\nu}$ varies between $\frac{\gamma_p}{\nu} = 1.501(1)$ for the decoupled Ising model and $\frac{\gamma_p}{\nu} = 1.750(4) \approx \frac{\gamma}{\nu}$ for the four-state Potts model. $\frac{\beta_p}{\nu}$ varies accordingly fulfilling the scaling relation (42).

Figures 13 and 14 show the critical χ_p and polarization P, respectively, as a function of $\ln L$ for the five critical models, $C_{0,...,4}$, of the RBAT. The same analysis has been carried out as for the AAT and the estimated critical exponents $\frac{\gamma_p}{\nu}$ and $\frac{\beta_p}{\nu}$ are listed in Table III. The results for the random-bond four-state Potts model C_4 agree with $P = M$ and $\chi_p = \chi$ to a high precision and thus need no further explanation.

There is a clear mismatch between the estimated values of $\frac{\gamma_p}{\nu}$ and $\frac{\beta_p}{\nu}$ and their expected values for the random-bond Ising model C_0. Even the left-hand side of the relation (40), $P = M^2$, which implied $\frac{\beta_p}{\nu} = 2\frac{\beta}{\nu}$, is far from being met, but rather we find $P > M^2$ both for
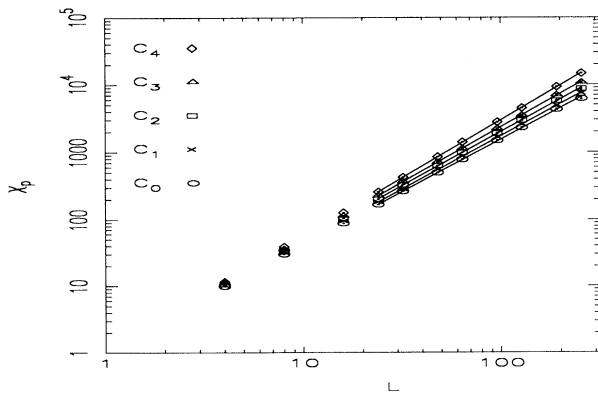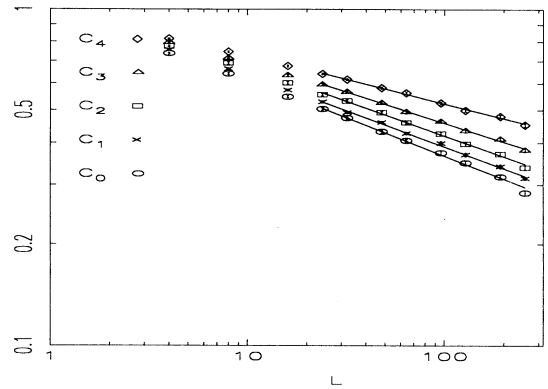
the anisotropic and for the random-bond Ising models. This is probably connected to the fact that we are measuring, as is usual in a MC calculation, $\langle |M| \rangle$ and $\langle |P| \rangle$ which are larger than $\lim_{h \to 0} \langle M \rangle$ and $\lim_{h_p \to 0} \langle P \rangle$ respectively. Both in the random-bond and anisotropic Ising models the relative variance of P is larger than the relative variance of M. This makes $\langle |P| \rangle$ a worse estimator of $\lim_{h_p \to 0} \langle P \rangle$ than $\langle |M| \rangle$ is of $\lim_{h \to 0} \langle M \rangle$. The discrepancy is a finite size effect [30] and should decay as L increases. Indeed if we estimate $\frac{\beta_p}{\nu}$ from lattices of size $L \geq 96$ we obtain $\frac{\beta_p}{\nu} = 0.266(22)$ which is consistent with the exact value $\frac{\beta_p}{\nu} = \frac{1}{4}$. An estimate of $\frac{\gamma_p}{\nu}$ from lattices of size $L \geq 64$ yields $\frac{\gamma_p}{\nu} = 1.524(23)$ which is consistent with the exact value $\frac{\gamma_p}{\nu} = \frac{3}{2}$.

The results for χ_p and P seem to favor a continuous variation of $\frac{\beta_p}{\nu}$ and $\frac{\gamma_p}{\nu}$ for the RBAT models as is the case for the AAT models. As explained above, for symmetry reasons one expects that if $\beta_{\text{Ising}} = \beta_{\text{Potts}}$ then $\beta_{p,\text{Ising}} \neq \beta_{p,\text{Potts}}$. This is consistent with the variation of exponents we find. Nonetheless since we found the specific heat of all models to diverge logarithmically one could expect the RBAT models to be more universal. A possible scenario to expect could be $\beta_p = \beta_{p,\text{Potts}}$ for all RBAT models but the Ising model. Then assuming $(\beta/\nu)_{\text{Ising}} = 1/8$ with (42) would imply $\frac{\gamma_p}{\nu} = 3/2$ for the Ising model and $\frac{\gamma_p}{\nu} = 7/4$ for all the other RBAT models. Such a behavior would of course be masqueraded by crossover, but nonetheless we do not find evidence for such a behavior in our results. Further investigation of this problem is clearly needed.

V. SUMMARY AND DISCUSSION

We have examined the effect of bond disorder on the line of critical points of the AT model. A duality transformation was used in order to locate a critical manifold of the random-bond AT model which corresponds to the line of critical points of the pure model. An anisotropic AT model was used as a convenient pure reference model. Our results consist of the finite size dependence of

FIG. 13. χ_p as a function of $\ln L$ for five critical models $C_{0,...,4}$, of the RBAT. The solid lines are linear fits to form (39b) for $L \geq 24$, yielding estimates for critical exponents $\frac{\gamma_p}{\nu}$ which are listed in Table III.

C, M, P, χ, and χ_p at criticality of several random-bond and anisotropic AT models. The models $C_{0,...,4}$ interpolate between Ising and four-state Potts models with large disorder, thus also monitoring the effect of changing the crossover exponent $(\alpha/\nu)_p$. The models A_2, B_2, and C_2 serve to monitor the effect of changing the amount of disorder while keeping the crossover exponent approximately the same $[0.37 \le (\alpha/\nu)_p \le 0.40]$.

The results of the critical specific heat of all the RBAT models agree very well with the crossover behavior (28), according to which for $L < L_c$, C diverges with the same exponent $(\alpha/\nu)_p$ as the corresponding AAT model, while for $L > L_c$, C grows as $\ln L$. Our estimates for the crossover lengths of the models A_2 and B_2 are much smaller than the estimates of Wang et al. for random-bond Ising models with the same amount of disorder. This is consistent with the Harris criterion and the crossover exponent $(\alpha/\nu)_p \approx 0.4$ of the former models, and the crossover exponent $(\alpha/\nu)_p = 0$ for the latter models. For the random-bond Ising model we find the double logarithmic divergence (31), or (33) asymptotically, as was found by Wang et al. We view the adequacy of (28) for all the RBAT models [with different $(\alpha/\nu)_p$ and different amounts of randomness] for the full lattice range $\le L \le 256$, together with the consistency of the crossover lengths with physical understanding (Harris criterion), as a strong indication that the RBAT models (including the four-state Potts model) exhibit a logarithmic divergence of C. We tend to rule out the possibility of a double logarithmic divergence of C as predicted by DD [27] for the Baxter model, for reasons explained in Sec. IV.

Although β/ν and γ/ν do not vary for the pure model, our results indicate a possibility that β/ν and γ/ν do vary for the random models. Nonetheless this very small variation might be an artifact of a correction to scaling, e.g., of a logarithmic type. The exponents connected with the polarization P and the susceptibilities χ_p, β_p/ν, and γ_p/ν which vary continuously for the pure AT model seem also to do so for the RBAT model. However, on the basis of universality the possibility that these exponents are actually the same (with some nonuniversal corrections to scaling and a crossover effect) for all RBAT models excluding the Ising model, seems to be a plausible scenario in need of further investigation.

Very recently an experimental study of a two dimensional four-state Potts system with quenched impurities

was done [45], and values of $\nu = 1.03(8)$, $\beta = 0.135(1)$, and $\gamma = 1.68(15)$ were obtained. These are consistent with our findings for the four-state Potts system C_4 but with a value of β which is smaller than ours.

APPENDIX: THE DUALITY TRANSFORMATION OF THE AT MODEL

We list here the duality transformation $\vec{D}[K, \Lambda]$ of the AT model and a few of its properties. For convenience, instead of (K, Λ) we use different variables for the coupling constants, (X, Z);

$$Z = \exp^{-4K}, \quad X = \exp^{-2(K+\Lambda)}, \quad \vec{X} = (X, Z). \quad (A1)$$

Under a duality transformation $\vec{D}$, a bond of strength $\vec{X} = (X, Z)$ transforms into a bond on the dual lattice of strength $\tilde{\vec{X}} = (\tilde{X}, \tilde{Z}) = \vec{D}(\vec{X})$ given by [34,20]

$$\begin{aligned} \tilde{X} &= (1 - Z)/\Delta, \\ \tilde{Z} &= (1 - 2X + Z)/\Delta, \quad (A2) \\ \Delta &= 1 + 2X + Z. \end{aligned}$$

We list several properties of the transformation. It is self-inverse, i.e., $\vec{D}[\vec{D}(\vec{X})] = \vec{X}$. It maps the zero temperature point $[\vec{X} = (0,0)]$ onto $T = \infty$ $[\vec{X} = (1,1)]$ and vice versa. The Ising subspace $Z = X^2$ and the four-state Potts subspace $Z = X$ are invariant under $\vec{D}$. The subspace Σ, defined by $X \ge Z \ge X^2$ (or $K \ge \Lambda \ge 0$), is also invariant under $\vec{D}$. The line $Z = 1 - 2X$ is a self-dual line, and its intersection with Σ is the line of critical points of the AT model. It is also true that if $Z \le 1 - 2X$ then $\tilde{Z} \ge 1 - 2\tilde{X}$ and vice versa.

[1] A. B. Harris, J. Phys. C, **71**, 1671 (1974).
[2] R. B. Stinchcombe, in *Phase Transitions and Critical Phenomena*, edited by C. Domb and J. L. Lebowitz (Academic, New York, 1983), Vol. 7.
[3] W. Kinzel and E. Domany, Phys. Rev. B **23**, 3421 (1981).
[4] T. C. Lubensky and A. B. Harris, in *Magnetism and Magnetic Materials 1974*, edited by C. D. Graham, Jr., G. H. Lander, and J. J. Rhyne, AIP Conf. Proc. No. 24 (AIP, New York, 1975), p. 311.
[5] C. Jayaprakash and H. J. Katz, Phys. Rev. B **16**, 3987 (1977).
[6] Vik S. Dotsenko and Vl S. Dotsenko, Adv. Phys. **32**, 129

(1983).
[7] B. N. Shalaev, Fiz. Tverd. Tela (Leningrad) **36**, 3002 (1984) [Sov. Phys. Solid State **26**, 1811 (1984)].
[8] R. Shankar, Phys Rev. Lett. **58**, 2466 (1987); **61**, 2390 (1988).
[9] A. W. W. Ludwig, Phys. Rev. Lett. **61**, 2388 (1988).
[10] W. Selke, in *Computer Simulations in Condensed Matter Physics III*, edited by D. P. Landau, K. K. Mon, and H. B. Schüttler (Springer, Heidelberg, 1991).
[11] D. Andelman and A. Nihat Berker, Phys. Rev. B **29**, 2630 (1984).
[12] B. Derrida and E. Gardner, J. Phys A **17**, 3223 (1984).

[13] A. W. W. Ludwig, Nucl. Phys. B **285**, 97 (1986).

[14] S. Chen, A. M. Ferrenberg, and D. P. Landau, Phys. Rev. Lett. **69**, 1213 (1992).

[15] A. N. Berker, Physica A **194**, 72 (1993).

[16] M. A. Novotny and D. P. Landau, Phys. Rev. B **24**, 1468 (1981).

[17] R. J. Baxter and F. Y. Wu, Phys. Rev. Lett. **31**, 1294 (1973).

[18] J. Ashkin and E. Teller, Phys. Rev. **64**, 178 (1943).

[19] F. Y. Wu and K. Y. Lin, J. Phys. C **7**, L181 (1974).

[20] E. Domany and E. K. Riedel, Phys. Rev. B **19**, 5817 (1979).

[21] R. V. Ditzian, J. R. Banavar, G. S. Grest, and L. P. Kadanoff, Phys. Rev. B **22**, 2542 (1980).

[22] S. Wiseman and E. Domany, Phys. Rev. E **48**, 4080 (1993).

[23] R. J. Baxter, *Exactly Solved Models in Statistical Mechanics* (Academic, London, 1982).

[24] B. Nienhuis, in *Phase Transitions and Critical Phenomena* (Ref. [2]), Vol. 11.

[25] F. C. Alcaraz and C. Tsallis, J. Phys. A **15**, 587 (1982).

[26] R. J. Baxter, Ann. Phys. (N.Y.) **70**, 193 (1972).

[27] Vik S. Dotsenko and Vl S. Dotsenko, J. Phys. A **17**, L301 (1984).

[28] D. Matthews-Morgan, D. P. Landau, and R. H. Swendsen, Phys. Rev. Lett. **53**, 679 (1984).

[29] For a review see, A. D. Sokal, Nuc. Phys. B **20**, 55 (1991).

[30] K. Binder and D. W. Heermann, *Monte Carlo Simulations in Statistical Physics* (Springer-Verlag, Berlin, 1988).

[31] H. O. Heuer, Phys. Rev. B **42**, 6476 (1990).

[32] J. S. Wang, W. Selke, VI. S. Dotsenko, and V. B. Andreichenko, Physica A **164**, 221 (1990).

[33] M. Hennecke and U. Heyken, J. Stat. Phys. **72**, 829 (1993).

[34] F. Y. Wu and Y. K. Wang, J. Math. Phys. **17**, 439 (1976).

[35] R. Fisch, J. Stat. Phys. **18**, 111 (1978).

[36] U. Wolff, Phys. Rev. Lett. **62**, 361 (1989).

[37] S. Caracciolo, R. G. Edwards, A. Pelissetto, and A. D. Sokal, Nuc. Phys. B **20**, 72 (1991).

[38] R. H. Swendsen and J. S. Wang, Phys. Rev. Lett. **58**, 86 (1987).

[39] V. B. Andreichenko, Vl. S. Dotsenko, W. Selke, and J.-S. Wang, Nucl. Phys. B **344**, 531 (1990).

[40] A factor of $k_B T$ has been omitted, but is irrelevant since all measurements are at a single temperature.

[41] U. Wolff, Nucl. Phys. B **300**, 501 (1988).

[42] A. D. Sokal, in *Computer Simulation Studies in Condensed Matter Physics: Recent Developments,* edited by D. P. Landau, K. K. Mon, and H.-B. Schüttler (Springer-Verlag, Berlin, 1988).

[43] M. N. Barber, in *Phase Transitions and Critical Phenomena* (Ref [2]), Vol. 8.

[44] X. J. Li and A. D. Sokal, Phys. Rev. Lett. **63**, 827 (1989).

[45] L. Schwenger, K. Budde, C. Voges, and H. Pfnür, Phys. Rev. Lett. **73**, 296 (1994).